Mon. Not. R. Astron. Soc. **000**, 1–10 (2002) Printed 9 December 2010 (MN LATEX style file v2.2)

Kepler observations of Am stars ⋆

L. A. Balona[1], V. Ripepi[2], G. Catanzaro[3], D. W. Kurtz[4], B. Smalley[5], P. De Cat[6], L. Eyer[7], A. Grigahcène[8], S. Leccia[2], J. Southworth[5], K. Uytterhoeven[9], H. Van Winckel[10], J. Christensen-Dalsgaard[11], H. Kjeldsen[11], D. A. Caldwell[12], J. Van Cleve[12], G. R. Forrest[13]

[1]*South African Astronomical Observatory, P.O. Box 9, Observatory 7935, Cape Town, South Africa*
[2]*INAF-Osservatorio Astronomico di Capodimonte, Via Moiariello 16, I-80131, Napoli, Italy*
[3]*INAF-Osservatorio Astrofisico di Catania, Via S.Sofia 78, I-95123, Catania, Italy*
[4]*Jeremiah Horrocks Institute of Astrophysics, University of Central Lancashire, Preston PR1 2HE, UK*
[5]*Astrophysics Group, Keele University, Staffordshire ST5 5BG, UK*
[6]*Koninklijke Sterrenwacht van Belgie, Brussels, Belgium*
[7]*Observatoire de Genéve, 51 ch. des Maillettes, CH-1290 Sauverny, Switzerland*
[8]*Centro de Astrofisica, Faculdade de Ciências,, Universidade do Porto, Rua das Estrelas, 4150-762 Porto, Portugal*
[9]*Laboratoire AIM, CEA/DSM CNRS-Université Paris Diderot, Paris, France*
[10]*Instituut voor Sterrenkunde, K.U. Leuven, Celestijnenlaan 200B, 3000 Leuven, Belgium*
[11]*Department of Physics and Astronomy, Building 1520, Aarhus University, 8000 Aarhus C, Denmark*
[12]*SETI Institute/NASA Ames Research Center, Moffett Field, CA 94035 USA*
[13]*Orbital Sciences Corporation/NASA Ames Research Center, Moffett Field, CA 94035, USA*

ABSTRACT
We present an analysis of high-resolution spectra for two pulsating Am stars in the *Kepler* field. The stellar parameters derived in this way are important because parameters derived from narrow-band photometry may be affected by the strong metal lines in these stars. We analyse the *Kepler* time series of ten known Am stars and find that six of them clearly show δ Scuti pulsations. The other four appear to be non-pulsating. We derive fundamental parameters for all known pulsating Am stars from ground-based observations and also for the *Kepler* Am stars to investigate the location of the instability strip for pulsating Am stars. We find that there is not much difference between the Am-star instability strip and the δ Scuti instability strip. We find that the observed location of pulsating Am stars in the HR diagram does not agree with the location predicted from diffusion calculations.

Key words: stars: chemically peculiar – stars: fundamental parameters – stars: oscillations – stars: variables: δ Scuti

1 INTRODUCTION

The study of pulsating stars in the δ Scuti instability strip has been rapidly developing over the last few years. Previous to space missions such as *MOST*, *CoRoT* and *Kepler*, we could separate the δ Sct stars from the cooler γ Dor stars purely on the basis of the frequencies. Ground-based observations of δ Sct stars showed that all have frequencies higher than about 5 d^{-1}. These are predominantly p modes driven by the κ mechanism operating in the partial ionization zone of HeII. γ Dor stars are located near the red edge of the δ Sct instability strip and have frequencies lower than 5 d^{-1}. These are g modes driven by the convective blocking mechanism.

A few stars showing characteristics of both types of variable were discovered and labelled as hybrid δ Sct/γ Dor pulsators. The presence of both types of modes in some models of these stars shows that convective blocking and κ mechanism can simultaneously drive low-frequency g modes and high-frequency p modes and explains the existence of the hybrids (Dupret et al. 2005). A significant part of the δ Sct instability strip overlaps the γ Dor instability strip and it is in this region where models show both low and high frequencies. The gap between the two frequency regimes is explained by radiative damping.

Results from *CoRoT* and particularly from *Kepler* have completely changed this picture. The lower detection limit from space observations shows that both high- and low-frequencies are present in almost all stars in the δ Sct instability strip (Grigahcène et al.

⋆ Based on observations made with the Italian Telescopio Nazionale Galileo (TNG) operated on the island of La Palma by the Fondación Galileo Galilei of the INAF (Istituto Nazionale di Astrofisica), at the Spanish Observatorio del Roque de los Muchachos of the Instituto de Astrofisica de Canarias, and with the Mercator Telescope operated on the island of La Palma by the Flemish Community.

2010). This means that it is no longer possible to distinguish between δ Sct and γ Dor stars on frequencies alone. The frequency gap predicted by the models does not exist. This problem remains unresolved at this stage.

The Ap stars are magnetic stars where the effect of diffusion in a magnetic field has left surface patches of different abundances. Vertical segregation of elements is also present. Our current understanding of diffusion is that He should drain from the ionization zone. When insufficient He remains in the driving region, the star cannot pulsate. On this basis, we would not expect to observe Ap stars with pulsations in the δ Sct frequency range. Furthermore, since Ap stars have strong magnetic fields, damping of pulsations due to magnetic slow wave leakage is also expected. The lack of δ Sct pulsations in Ap stars is indeed supported by ground-based observations where so far only one Ap star is known to be a δ Sct variable (Koen et al. 2001). However, *Kepler* observations of Ap stars indicate that pulsation in Ap stars may be more common than expected (Balona et al. 2010).

Note that driving of the high-frequency pulsations in roAp stars is not connected with helium, but appears to be due to the opacity bump in the hydrogen ionization zone. Pulsational instability occurs when convection in this zone is suppressed by a magnetic field. Thus the effect of diffusion is quite different in this case.

Closely related to the Ap stars are the metallic-lined A stars, the Am stars. These are A-type stars (judging by the strength of the Balmer lines), but with strong absorption lines of some metals such as Zn, Sr, Zr and Ba and weaker lines of other metals such as Ca and/or Sc (Preston 1974). The strengths of these metal lines are more typical of an F star rather than an A star. It is thought that these anomalies are a result of diffusion in a non-magnetic star. A peculiarity of Am stars is that their projected rotational velocities are generally smaller than normal A stars ($v \sin i$ typically less than 100 km s^{-1}) and that the vast majority of Am stars are known to be members of close binary systems. Rotational braking by tidal friction in a binary system is regarded as a possible explanation for the low rotational velocities of Am stars. Slow rotation further assists the segregation of elements by diffusion.

For many years it was thought that Am stars did not pulsate, in accordance with the expectation of diffusion which depletes helium from the driving zone. More intensive observations have revealed that this picture is not correct and several Am stars are known to pulsate from ground-based observations. The diffusion scenario has been modified to include diffusion of heavy elements (Turcotte et al. 2000). This new model makes certain predictions regarding the location of pulsating Am stars in the HR diagram which can be tested.

In this context, data from the *Kepler* satellite can provide important information on the incidence of pulsation in Am stars. Because *Kepler* photometry attains a precision of only a few μmag even for rather faint stars, lack of variability due to pulsation cannot be attributed to insufficient detector sensitivity. It may then be possible to falsify current theories regarding diffusion in Am stars if pulsation is detected outside the region in the HR diagram where theory dictates that pulsation should not occur. There are 10 known Am stars in the *Kepler* field of view, which is a reasonable sample for this purpose. An overview of the *Kepler* science processing pipeline is presented by Jenkins et al. (2010).

Of course, it is necessary to place these stars in the HR diagram, and for this purpose high-resolution spectroscopy is the best tool. Because of the blanketing caused by the chemical peculiarities in the atmospheres of Am stars, fundamental stellar parameters based on photometric indices may not be appropriate for Am stars. This problem can only be resolved by matching synthetic spectra to the observed spectra of Am stars. For this purpose, we present an analysis of two *Kepler* Am stars: KIC 11402951 and KIC 11445913. The only previous investigation of these two Am stars is the recent preliminary analysis by Catanzaro et al. (2010) and observations by Abt (1984) who obtained photographic spectra with 1 Å resolution for classification purposes. A spectroscopic analysis of a third *Kepler* star, KIC 7548479, is already available (Antoci et al. 2010).

Using these results, we discuss how the ten pulsating and non-pulsating Am stars observed by *Kepler* can help us understand the diffusion process in these stars. We supplement these results with data from all known pulsating Am stars from ground-based observations and compare the instability region for these stars with that calculated from recent Am star models incorporating heavy-element diffusion.

Table 1. Radial velocities (km s^{-1}) for KIC 11445913. The truncated heliocentric Julian day (HJD - 245000.0) is given. The last column shows the observatory where spectra were obtained as follows: OAC - Catania Astrophysical Observatory, TNG - Telescopio Nazionale Galileo, Her - Hermes, McD - McDonald Observatory.

HJD	$V_{\rm rad}$	Obs
5104.4784	-35.0 ± 1.7	OAC
5141.3271	-34.1 ± 1.3	TNG
5309.5687	-26.2 ± 0.5	Her
5370.7018	-21.9 ± 2.5	McD
5371.6582	-21.3 ± 3.1	McD
5372.6497	-21.8 ± 3.6	McD
5373.7117	-22.6 ± 3.0	McD
5376.6495	-24.3 ± 6.7	McD

2 SPECTROSCOPIC OBSERVATIONS

SARG is a high-resolution cross-dispersed echelle spectrograph (Gratton et al. 2001) that operates in both single-object and longslit modes (with up to 26 slits). The spectra cover the wavelength range from 3700 Å up to about 10000 Å with a resolution ranging from R = 29 000 to 164 000.

Spectra were obtained on 2009, November 5[1] at R = 57 000 with exposure times of 600 s using two grisms (blue and yellow) and two filters (blue and yellow). These were used in order to obtain a continuous spectrum from 3600 Å to 7900 Å with significant overlap in the wavelength range between 4620 Å and 5140 Å. We analysed the spectral region 4600 — 6100 Å where the signal-to-noise (S/N) is largest ($60 < \mathrm{S/N} < 140$). In the region centered around the MgI triplet at 5170 Å the measured S/N is about 80.

One spectrum of KIC 11445913 was acquired on 2010 April 22 with the HERMES@Mercator telescope. The spectral range is 4000 – 9000 Å with S/N at least 150 and resolving power R $\approx$ 85 000. Five further spectra of this star were obtained with the Sandiford Cassegrain Echelle Spectrometer mounted on on the 2.1-m Otto Struve Telescope at McDonald Observatory, Texas, USA. Spectra were obtained between 2010 June 22 – 28, with a resolving power of R $\approx$ 60 000. Depending on conditions, the S/N varies from 80 – 250. The reduction of all spectra was done using

[1] Director Discretionary Time, proposal ID: A20DDT5

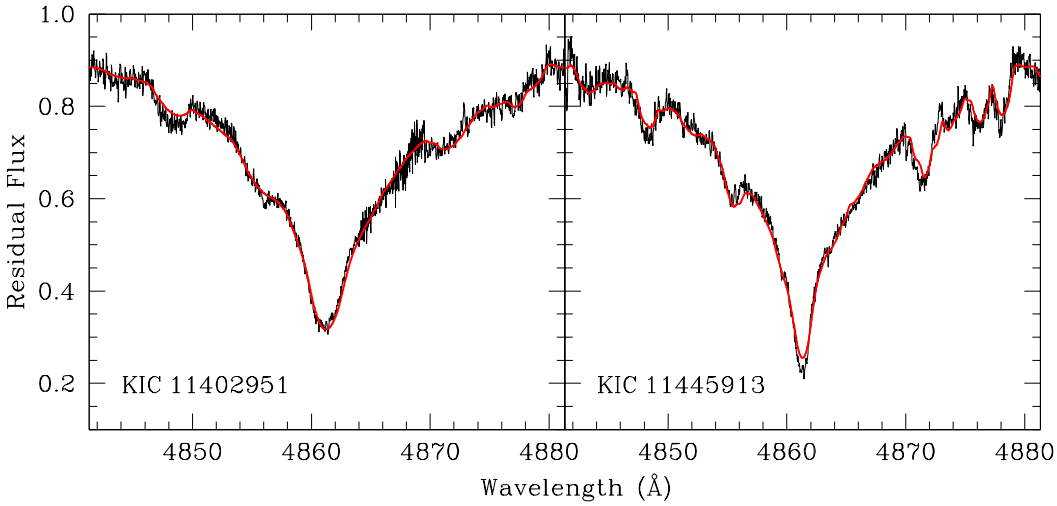

Figure 1. Observed and synthetic Hβ line profiles for two *Kepler* Am stars. Fundamental parameters for the synthetic line profiles are given in Table 2.

Table 2. Data for two *Kepler* Am stars discussed in this paper. $T_{\rm eff}$(lit) (in K) is from Catanzaro et al. (2010) and $T_{\rm eff}$(TNG) is from the Hβ observations with SARG@TNG. $T_{\rm eff}$ is the finally adopted effective temperature, while $\log g$ and $v \sin i$ are the surface gravity (cgs units) and projected rotational velocity (km s^{-1}) derived from the spectra.

Quantity	KIC 11402951	KIC 11445913
V (mag)	8.14	8.46
$T_{\rm eff}$(lit)	7150 ± 120	7200 ± 120
$T_{\rm eff}$(TNG)	7400 ± 150	7400 ± 200
$T_{\rm eff}$	7250 ± 100	7250 ± 100
$\log g$	3.5 ± 0.1	3.5 ± 0.2
$v \sin i$	100 ± 2	51 ± 1

the NOAO/IRAF packages[2]. The IRAF package rvcorrect was used to correct times to the heliocentric rest frame.

Since quite a few spectra taken at different times are available for KIC 11445913, we decided to investigate the radial velocity variation using the fxcor cross-correlation code in IRAF. For this purpose, we also included a spectrum obtained at the INAF-Catania Astrophysical Observatory which was previously used in the analysis of Catanzaro et al. (2010). The resulting radial velocities are shown in Table 1. These are clustered in two groups spanning about 10 km s^{-1}, suggesting that KIC 11445913 is probably a single-lined spectroscopic binary. Nearly all Am stars are members of binary systems so this result is not surprising.

3 PHYSICAL PARAMETERS

We determined the effective temperature, $T_{\rm eff}$, and surface gravity, $\log g$, of the stars by minimizing the difference between the observed and the synthetic Hβ line profiles. For the goodness-of-fit parameter, we used χ^2 defined as

$$\chi^2 = \frac{1}{N} \sum \left(\frac{I_{\rm obs} - I_{\rm th}}{\delta I_{\rm obs}} \right)^2 ,$$

where N is the total number of points, $I_{\rm obs}$ and $I_{\rm th}$ are the intensities of the observed and computed profiles respectively, and $\delta I_{\rm obs}$ is the photon noise. The standard deviation of a particular quantity can be calculated from the deviation which will increase χ^2 by unity. The values of $T_{\rm eff}$, $\log g$, and $v \sin i$ in Catanzaro et al. (2010) were used as starting values for the solution. The projected rotational velocity was estimated by matching the metallic line profiles in the range 5160 - 5200 Å with synthetic profiles. In this spectral range, the MgI triplet at 5167.321, 5172.684, and 5183.604 Å is a very useful diagnostic for surface gravity. The value of $\log g$ from these lines was used to check the reliability of $\log g$ determined from the Hβ line profile fit.

We have adopted the weighted mean of the effective temperatures and gravities determined in this study and in Catanzaro et al. (2010) as final values. These results are shown in Table 2. Note that the projected rotational velocity of 100 km s^{-1} for KIC 11402951 is among the highest for an Am star. In Fig. 1, we show the match between the data and the synthetic Hβ line profiles. The synthetic line profiles were computed with SYNTHE (Kurucz & Avrett 1981) using ATLAS9 (Kurucz 1993) atmospheric models. All models were calculated using the solar opacity distribution function and a microturbulence velocity $\xi = 3$ km s^{-1}. This value was determined from the $\xi = \xi(T_{\rm eff}, \log g)$ calibration in Allende Prieto et al. (2004).

High-dispersion spectroscopy gives values of $\log T_{\rm eff}$ and $\log g$, but we need $\log L/L_\odot$ to place the star in the HR diagram. One way to do this is simply to use $\log g$ as an indicator of spectral class and use a calibration of spectral type as a function of luminosity to obtain $\log L/L_\odot$. This is the method used in Catanzaro et al. (2010). Evolutionary models give us $\log T_{\rm eff}$, $\log L/L_\odot$ and $\log g$ for a given mass and composition, so one can select a model which matches the $\log T_{\rm eff}$, $\log g$ value to directly obtain $\log L/L_\odot$ with much better precision.

[2] IRAF is distributed by the National Optical Astronomy Observatory, which is operated by the Association of Universities for Research in Astronomy, Inc.

We can also dispense with evolutionary models altogether and use a purely empirical mass-luminosity relationship. We use $L/L_\odot = (R/R_\odot)^2 (T_{\rm eff}/T_{\rm eff\odot})^4$ together with $g/g_\odot = \left(M/M_\odot\right) / (R/R_\odot)^2$ to eliminate the stellar radius, R. This leaves us with a relationship expressing the luminosity in terms of the effective temperature, gravity and mass. The mass can be eliminated using a suitable mass-luminosity relationship, giving $\log L/L_\odot$ in terms of $\log T_{\rm eff}$ and $\log g$. We used the relationship in Torres et al. (2010).

Since reliable determination of the atmospheric parameters of Am stars can be somewhat problematical (Smalley & Dworetsky 1993), we have used available broad-band photometry and Strömgren $uvby$ photometry as an independent check on our spectroscopic determinations. Spectral energy distributions constructed using broad-band photometry from the literature were fitted using Kurucz (1993) model fluxes to estimate values of $T_{\rm eff}$, which are generally in reasonable agreement with the values listed in the *Kepler Input Catalogue* (KIC) and those from spectroscopy. For the four *Kepler* Am stars that have $uvby$ photometry we have used the calibration of Balona (1994) and the grids of Smalley & Kupka (1997) to determine $T_{\rm eff}$ and $\log g$, with luminosity estimated using the calibration of Torres et al. (2010). These luminosity values are in accord with those determined for stars with measured parallaxes (van Leeuwen 2007), but somewhat discrepant with those from spectroscopy due to differences in $\log g$ of up to 0.5 dex.

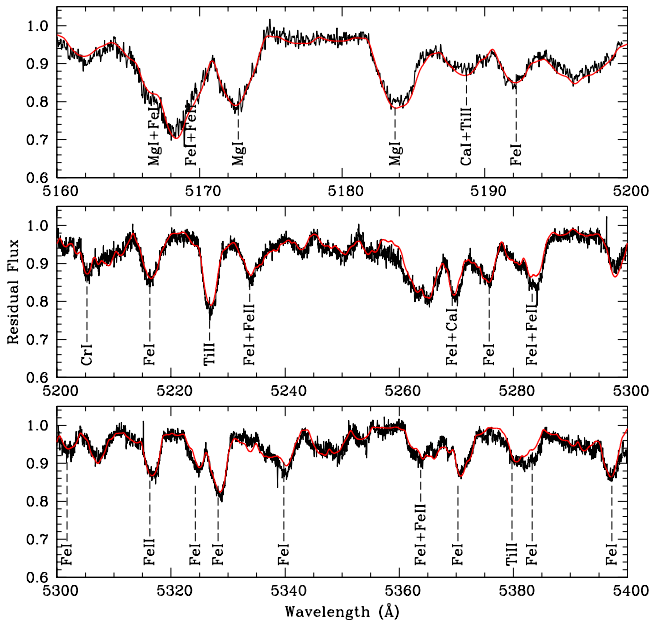

Figure 2. Spectral interval between 5160 and 5400 Å of KIC 11402951 observed with the SARG spectrograph superimposed on the computed model

4 METAL ABUNDANCES

The spectral lines in the two *Kepler* Am stars are relatively broad and it is difficult to find unblended lines. To overcome this problem, the stellar abundance was estimated by matching a rotationally-broadened synthetic spectrum to the observed spectrum. For this purpose we divided the spectrum into separate wavelength segments each covering a range of 25 Å. For each segment, the abundance was determined by χ^2 minimization. We used the spectral line list and atomic parameters in Castelli & Hubrig (2004) which are updated from Kurucz & Bell (1995).

One can calculate the mean abundance of a particular element from the individual abundances in each segment. The standard deviation of the mean can also be calculated. The standard deviation of the mean calculated in this way was taken as the overall standard deviation for the abundance of the element in question. For elements whose lines occurred in only one or two segments, the error in the abundance was evaluated by varying the effective temperature and gravity within their uncertainties (as given in Table 2) and computing the abundance for $T_{\rm eff}$ and $\log g$ values within these ranges. We found a variation of ≈ 0.1 dex in abundance due to temperature variation, but no significant variation when $\log g$ was varied. Thus the uncertainty in temperature is probably the main source of error in the abundance. In Figs 2 and 3 we show examples of the matching between synthetic and observed spectra. The abundances are given in Table 3.

In Fig. 4 we show a comparison between the abundances derived for our targets and the solar values in Grevesse et al. (2010). A comparison with the abundances of normal stars of the same spectral type is also shown. To do this, we extracted a homogeneous sample of abundances for A-type stars with $7000 \leqslant T_{\rm eff} \leqslant 8000$ K and $3.5 \leqslant \log g \leqslant 4.0$ from the list of Erspamer & North (2003) (a total of 42 stars). We used the average abundance for each element in these stars as a representative abundance. The standard deviation

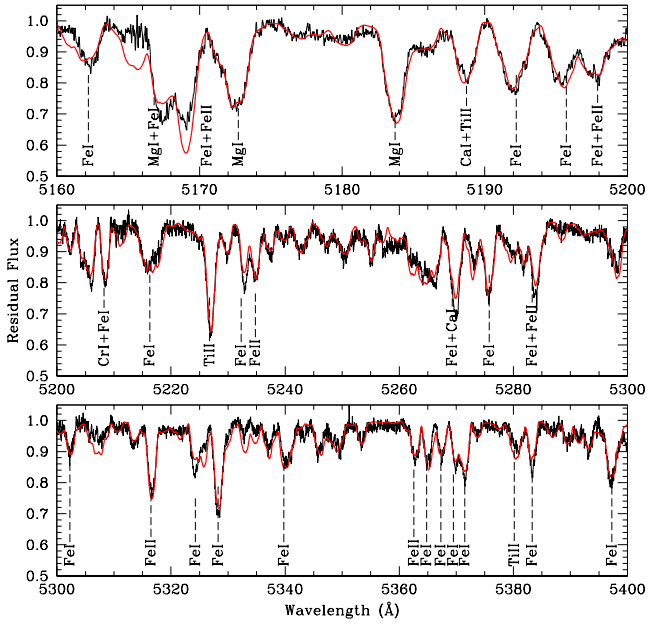

Figure 3. As Fig. 2 but for KIC 11445913

of the representative abundance was determined from the scatter in abundances.

Classical Am stars are defined as A-type stars in which the spectral type from the Ca K line and the spectral type from other metal lines differ by five or more spectral subclasses. In the two Am stars, KIC 11402951 and KIC 11445913, we find a slight overabundance of iron-peak elements such as Ti, Fe and Ni ($\leqslant 0.8$ dex). In KIC 11445913 there is also an overabundance of Ba (≈ 1 dex).

Table 4. Am stars observed by *Kepler*. The spectral classification from the literature is given in the third column. The columns marked Long and Short give the time span of the observations in days for long- and short-cadence exposures. The last two columns give the derived effective temperatures and luminosities.

KIC	Name	Classification	Long	Short	$\log T_{\rm eff}$	$\log L/L_\odot$
3429637	HD 178875	kF2hA9mF3	310.6	—	3.843[a]	1.54[a],1.67[b],1.50[d]
5219533	HD 226766	kA2hA8mA8	9.7	33.4	3.870[a]	1.08[a]
7548479	HD 187547	Am	44.4	30.4	3.875[a]	1.31[c]
8323104	HD 188911	kA2mF0	44.4	30.4	3.880[a]	1.15[a]
8703413	HD 187254	kA2mF0	44.4	25.9	3.887[a]	1.36[a]
9117875	HD 190165	kA2mF2	33.4	9.7	3.865[e]	0.90[b]
9204718	HD 176843	kA3mF0	44.4	25.9	3.854[a]	1.01[a]
9272082	HD 179458	Am?	44.4	29.9	3.929[d]	1.32[d]
11402951	HD 183489	kF3hA9mF5	228.9	9.7	3.860[c]	1.68[c], 1.11[c], 1.07[d]
11445913	HD 178327	kA7hA9mF5	228.9	9.7	3.842[a],3.860[c]	1.01[a], 1.68[c], 0.90[d]

[a] From the KIC catalogue. [b] From Hipparcos parallaxes. [c] From high-dispersion spectroscopy. [d] From $uvby\beta$ and Balona (1994) and Smalley & Kupka (1997). [e] From broad-band photometry.

Table 3. Abundances inferred for the two stars of our sample expressed in the form $\log N/N_{\rm tot}$. For comparison we report the abundances of the Sun (Grevesse et al. 2010) and of the A-type stars (Erspamer & North 2003)

El.	KIC 11402951	KIC 11445913	Sun	A type
C	—	-3.52 ± 0.20	-3.62 ± 0.05	-3.54 ± 0.08
Na	-5.50 ± 0.10	-5.50 ± 0.20	-5.79 ± 0.04	-5.35 ± 0.12
Mg	-4.00 ± 0.10	-4.05 ± 0.10	-4.43 ± 0.04	-4.33 ± 0.13
Si	-4.50 ± 0.10	-4.40 ± 0.20	-4.52 ± 0.03	-4.42 ± 0.06
Ca	-5.70 ± 0.20	-5.70 ± 0.20	-5.69 ± 0.04	-5.69 ± 0.09
Sc	-8.70 ± 0.10	-8.80 ± 0.20	-8.88 ± 0.04	-8.60 ± 0.15
Ti	-6.30 ± 0.25	-6.75 ± 0.10	-7.08 ± 0.05	-7.05 ± 0.10
Cr	-6.10 ± 0.20	-6.15 ± 0.20	-6.39 ± 0.04	-6.40 ± 0.12
Mn	-6.65 ± 0.20	-6.10 ± 0.15	-6.60 ± 0.04	-6.59 ± 0.13
Fe	-4.00 ± 0.10	-4.00 ± 0.20	-4.53 ± 0.04	-4.56 ± 0.11
Ni	-4.95 ± 0.15	-5.60 ± 0.10	-5.81 ± 0.04	-5.81 ± 0.13
Sr	—	-9.25 ± 0.10	-9.16 ± 0.07	-8.89 ± 0.34
Y	-9.30 ± 0.20	-9.25 ± 0.10	-9.82 ± 0.05	-9.39 ± 0.15
Ba	-9.40 ± 0.10	-8.85 ± 0.10	-9.85 ± 0.09	-9.48 ± 0.18

The abundances of Ca and Sc appear to be normal. This is unusual, but not unknown among Am stars.

Abt (1984) classifies KIC 11402951 as kF3hA9mF5 and KIC 11445913 as kA7hA9mF5, indicating that while the strength of the Balmer lines indicates a spectral type of A9, the metal lines indicate a spectral type of F5 in both stars. Indeed, we find that the metal lines can be quite well matched in a solar abundance model with effective temperature of about 6500 K which corresponds to F5 (though the fit to the Hβ line is very poor, of course). This supports the classification of these two stars as classical Am stars.

5 *KEPLER* OBSERVATIONS OF Am STARS

The *Kepler Mission* is designed to detect Earth-like planets around solar-type stars using the transit method (Koch et al. 2010). To achieve that goal, *Kepler* is continuously monitoring the brightness of over 150 000 stars for at least 3.5 yr in a 105 square degree fixed field of view. The resulting photometry allows the detection of pulsation amplitudes of just a few μmag. The *Kepler* observations consist mostly of exposures of approximately 30 min duration (long cadence), but a small allocation for short-cadence (1-min) exposures is available. Long-cadence exposures are only able to detect

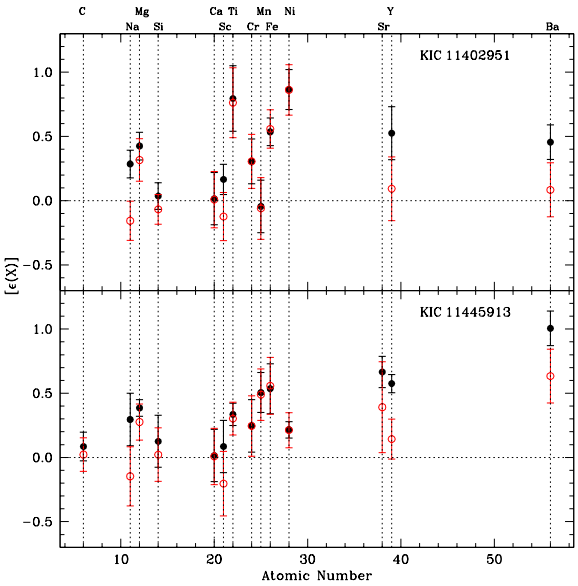

Figure 4. Abundance patterns derived for two *Kepler* Am stars (see Table 3). Filled circles (black) show abundances relative to the solar values, while open circles (red) show abundances relative to a sample of A-type stars.

frequencies lower than about 24 d^{-1} making them less useful for studying pulsations in the δ Sct frequency range. As an indication of the quality of the data, we show in Fig. 5 part of the light curves of the two *Kepler* Am stars for which we obtained high-resolution spectroscopy.

The known Am stars which are accessible to *Kepler* are listed in Table 4. All stars except KIC 3429637 were observed in short-cadence mode. Most of the stars were observed during the survey phase and the short-cadence runs have durations of about 10 or 30 d, but some of the stars have been observed for a much longer time in long-cadence mode. There are, no doubt, a great many *Kepler* stars which may be Am stars but for which no spectroscopy is available. One such star for which high-dispersion spectroscopy has recently been obtained is KIC 7548479 (Antoci et al. 2010).

The periodograms of these stars are shown in Figs. 6. We notice that while some stars definitely show pulsations in the δ Sct

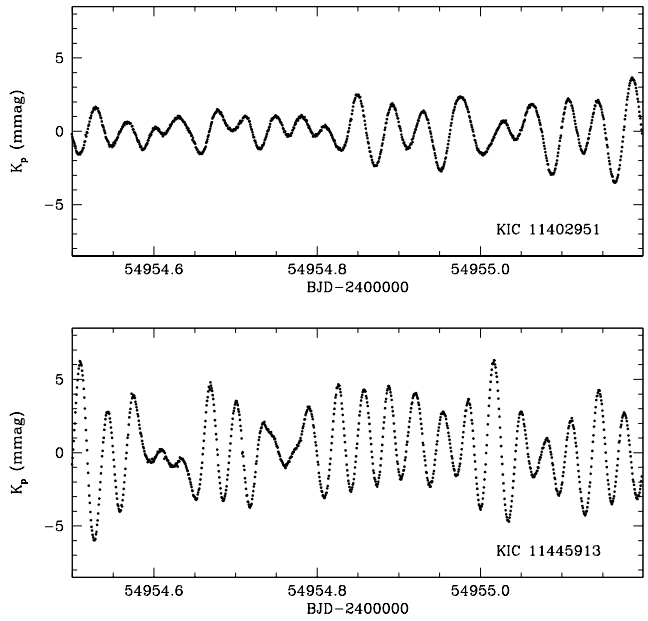

Figure 5. Selected portion of light curves for the two *Kepler* Am stars for which we obtained high-resolution spectra. Note the very high S/N of the data.

region, others only show variability at much lower frequencies. We note that the two Am stars that we have studied with high-resolution spectroscopy both have very rich frequency spectra. KIC 11445913 would be classified as a δ Sct/γ Dor hybrid. On the other hand KIC 11402951 has only very low amplitude signals in the low-frequency range. Of the other stars, KIC 3429637, KIC 7548479, KIC 9204718 and KIC 5219533 (another hybrid) show clear δ Sct pulsations. The other Am stars do not show anything significant in the δ Sct range, though clear low-frequency variability is present in most cases. Some of this low-frequency variability may be of instrumental origin as long-term trends in *Kepler* data are not fully corrected. However, intrinsic variability could arise as a result of rotational modulation, for example. While no Am star is known to vary in this way from ground-based observations, it cannot be ruled out in *Kepler* photometry due to the extraordinary high precision.

What we want to do is to place the Am stars in the HR diagram as accurately as possible to see if there is a particular region for Am-star pulsation. As already mentioned, the most reliable parameters are those from high-dispersion spectroscopy, but there are only five pulsating Am stars where such parameters are available. Other pulsating Am stars have good *Hipparcos* parallaxes and these too are important since their luminosities can be reliably estimated even if the effective temperatures are less certain. The stars in these two categories are listed in Table 5.

The KIC lists effective temperatures and radii for most stars derived from the Sloan-like filters. The resulting values of $\log \mathrm{T_{eff}}$ and $\log \mathrm{L/L_\odot}$ are shown in Table 4. For stars with available Strömgren photometry (Table 6), the temperature and luminosity can be derived using the calibrations in Balona (1994). The stars in these two categories have less reliable parameters and should be given less weight than the stars in Table 5.

Due to the extraordinary photometric precision of *Kepler*, we can be practically certain that the non-pulsating *Kepler* stars are indeed non-pulsating. This is not the case for ground-based observations of Am stars. Non-detection of pulsation in this case could just mean that the pulsational amplitude is below one millimag, the typical threshold for ground-based photometry. Therefore, the location in the HR diagram of Am stars which are deemed to be non-pulsating from ground-based observations is not very useful.

It is, however, important to include ground-based data of pulsating Am stars to improve the statistics. For this purpose, we show in Table 6 pulsating Am stars with $uvby\beta$ photometry and derive the effective temperatures and luminosities using the Balona (1994) calibration. Note that HD 114839 in this Table was observed by the MOST satellite (King et al. 2006). We have also included some preliminary results from (Smalley et al., in preparation) who identified around 200 pulsating Am stars using the photometry from the SuperWASP exoplanet survey (Pollacco et al. 2006).

The typical standard deviation of $\mathrm{T_{eff}}$ obtained from spectroscopic measurements is about 200 K which contributes to a standard deviation of about 0.01 in $\log \mathrm{L/L_\odot}$. The spectroscopic value of $\log g$ has a typical standard deviation of about 0.1–0.2 which leads to a standard deviation of 0.2–0.3 in $\log \mathrm{L/L_\odot}$. The standard deviation of $\mathrm{T_{eff}}$ from Strömgren photometry is in the range 100–400 K (Balona 1994), but there might be a unknown systematic error for Am stars, of course. The standard deviation in the absolute magnitude derived for A-F stars is typically 0.3–0.4 mag which is about 0.15–0.20 in $\log \mathrm{L/L_\odot}$. Overall, we may attach a standard deviation of about 0.01 in $\log \mathrm{T_{eff}}$ and 0.2–0.3 in $\log \mathrm{L/L_\odot}$.

We show the resulting location of the constant and pulsating Am stars in Fig. 7. Whenever possible we use parameters from Table 5, failing this we use parameters from Table 6 and lastly the KIC parameters in Table 4. There does not appear to be a systematic difference between stars with spectroscopic or parallax measurements and those whose parameters were determined from the KIC or $uvby\beta$ photometry. Besides the Am stars, we show in this diagram all known *Kepler* δ Sct stars (using parameters in the KIC) as well as δ Sct stars from ground-based observations for which the parameters can be derived using $uvby\beta$ photometry and the Balona (1994) calibration.

6 DISCUSSION

The question of why the atmospheres of Am stars are enriched in metals is not fully understood. In Am and Ap stars, the observed abundance anomalies are thought to develop as a consequence of diffusion in which He sinks and metals rise. In A and F stars there are two thin convective regions just below the photosphere in which H and HeII are partially ionized. In non-magnetic stars these two convective zones merge to form a single convective layer. As He drains from the envelope due to diffusion, the opacity in this joint convective layer drops, resulting in a much thinner layer supported by ionization of hydrogen. As a consequence, the opacity bump is modified and pulsation can no longer be driven. The study of pulsation among Am stars can tell us about the opacity in envelope, providing information and a probe of diffusion in these stars.

It turns out that if only the diffusion of helium is considered, models predict a much larger over-abundance of heavy elements than actually observed. This problem appears to be solved if diffusion of heavy elements is also taken into account (Turcotte et al. 2000). As heavy elements settle, the deeper iron-bump opacity region at about 2×10^5 K is enriched by these elements, which increases the opacity. As a result, a convective zone develops in this region. This new convective zone, which lies below the thin con-

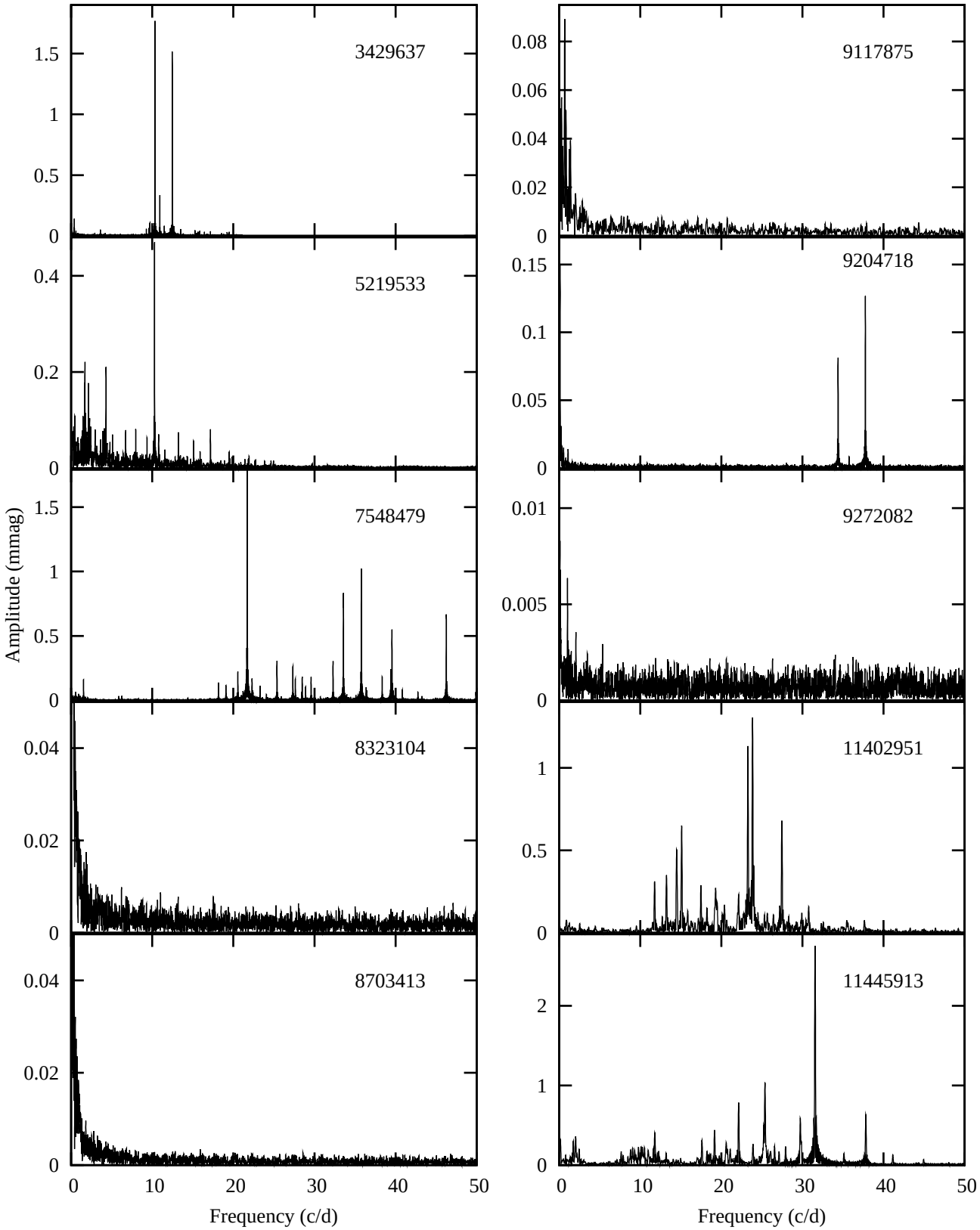

Figure 6. Periodograms of Am stars from *Kepler* photometry. The numbers in the panels refer to the KIC identifications.

Table 5. Am stars which have very good trigonometric parallaxes (P) or good spectroscopic parameters (S). Effective temperatures, $T_{\rm eff}$ are in K and surface garvity, g, in cm s^{-2}.

HD	Classification	$\log T_{\rm eff}$	$\log g$	$\log L/L_\odot$	Type	Reference
8801	kA5hF1mF2	3.855	4.20	0.80	S	Henry & Fekel (2005)
27628	kA5hF0mF2	3.864	4.00	1.04	P	Burkhart & Coupry (1989)
71297	A5III-IV	3.900	4.19	1.14	P	Allende Prieto & Lambert (1999)
98851	kF1hF1IVmF3	3.845	3.50	1.67	S	Joshi et al. (2003)
102480	kF2hF4mF4	3.843	3.11	2.18	S	Robinson et al. (2007)
104513	A7m	3.879	4.24	0.88	P	Allende Prieto & Lambert (1999)
178327	kA7hA9mF5	3.860	3.50	1.75	S	KIC 11445913
183489	kF3hA9mF5	3.860	3.50	1.75	S	KIC 11402951
187547	Am	3.875	3.90	1.30	S	Antoci et al. (2010)
199434	F5II-III	3.825	—	1.57	P	Hohle et al. (2010)
204188	kA6hA9mF0	3.898	4.34	0.89	P	Allende Prieto & Lambert (1999)

Table 6. Pulsating Am stars not in the *Kepler* field. The effective temperatures and luminosities are derived from published $uvby\beta$ photometry and the Balona (1994) calibration. References to the pulsational nature are shown in the last column.

HD	Classification	$\log T_{\rm eff}$	$\log L/L_\odot$	Reference
1097	A3/5mF0-F5	3.880	0.11	Kurtz (1989)
8801	kA5hF1mF2	3.868	0.75	Henry & Fekel (2005)
13038	A4m	3.911	0.76	Martinez et al. (2001)
13079	Am	3.874	0.62	Martinez et al. (2001)
27628	kA5hF0mF2	3.872	0.81	Zhiping (2000)
71297	A5III-IV	3.907	0.81	Kurtz (1984)
104513	A7m	3.879	0.87	Kurtz (1978)
113878	kA5hF0mF3	3.865	0.91	Joshi et al. (2006)
114839	kA5mF0	3.879	0.72	King et al. (2006)
118660	A1 IV	3.883	0.96	Joshi et al. (2006)
204188	kA6hA9mF0	3.898	0.74	Kurtz (1978)

vective zone of partial hydrogen ionization, is assumed to mix with the hydrogen convection zone by overshooting. The result is a single, thicker, convective zone in which the abundance anomalies are diluted. In this way, the calculated abundances are in better agreement with observations.

The inclusion of heavy element diffusion also leaves a substantial amount of helium in the HeII driving region and increases the iron-bump opacity. Thus pulsational driving may result in certain regions of the HR diagram. In this scenario, the effect of diffusion on pulsation is to reduce the width of the instability strip, with the blue edge shifting towards the red edge, eventually leading to the disappearance of instability when helium is sufficiently depleted from the HeII ionization zone (Turcotte et al. 2000). The amount of driving is related to the amount of helium still present in the convective envelope and therefore to the depth of the convective envelope. The cooler the star, the deeper the convective envelope and the larger the driving. This is the physical reason why the blue edge moves towards cooler temperature in these Am star models.

Another effect of diffusion is that driving from the ionization of iron-group metals increases relative to driving from HeII ionization. As a consequence, it turns out that the pulsation frequency depends on the depth of the HeII ionization zone. As the star evolves, the depth of this zone increases and the frequencies decrease (Turcotte et al. 2000). It is found that models of young Am stars near the ZAMS are stable, while those of δ Sct stars of the same age pulsate. Models of Am stars eventually become pulsationally unstable as the star evolves, whereas standard δ Sct models remain pulsationally unstable throughout.

According to the hypothesis described above, one may expect to find pulsating Am stars near the cool edge of the instability strip. Neither hot Am stars nor Am stars near the ZAMS should pulsate (Turcotte et al. 2000). The blue edge of the instability strip for Am stars depends on the over-abundance factor. In models representative of Am stars, turbulence is high enough to prevent the development of convection in the Fe-bump opacity region while allowing a significant increase of the Fe-bump opacity. This has the marginal effect of destabilizing some high radial overtone g modes. The higher-frequency modes depend mostly on the He abundance and to a lesser extent on the H abundance as well. Fig. 7 shows the approximate maximum extent of the instability region for Am stars according to Turcotte et al. (2000). At that time, it was thought that the majority of Am stars do not pulsate, but that evolved Am stars (the δ Del stars) do pulsate. Reasonable agreement between the location of pulsating δ Del stars and the predicted instability strip was found.

From Fig. 7 we see that the pulsating *Kepler* Am stars occupy more or less the same region as normal δ Sct stars. There are several pulsating Am stars with parameters determined by spectroscopy or parallaxes that are well outside the predicted instability strip. In fact, the more evolved Am stars, which includes both

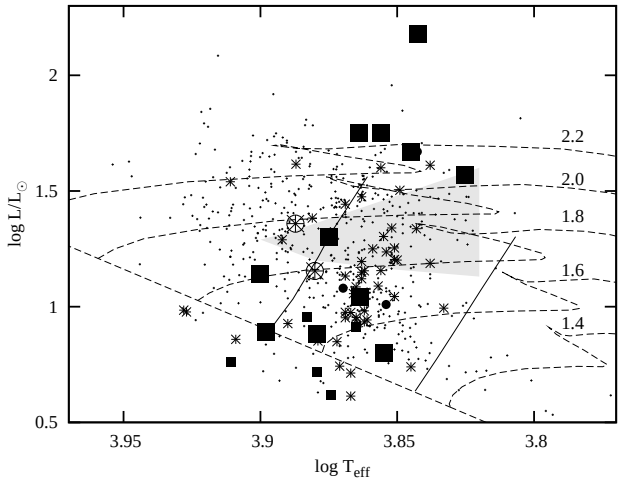

Figure 7. Location of Am stars in the theoretical HR diagram. Filled circles are *Kepler* pulsating Am stars and filled squares are other pulsating Am stars. The larger symbols are the stars for which parameters were determined from spectroscopy or parallaxes. Crossed open circles are two non-pulsating *Kepler* Am stars (KIC 188911 and KIC 187254). The asterisks are pulsating Am stars from SuperWASP observations. The gray area is the approximate location of pulsating Am-star models incorporating heavy-metal diffusion. The small background points are known δ Sct stars from ground-based observations and from *Kepler*. Evolutionary tracks (from Duprt et al. 2004) are shown for the indicated masses. Also shown are the fundamental radial mode red and blue edges from Dupret et al. 2004.

KIC 11402951 and KIC 11445913, are quite close to the theoretical radial fundamental blue edge. On the other hand, the two non-pulsating Am stars in *Kepler* do seem to be hotter than the pulsating Am stars, but we are dealing here with very small numbers. It would be important to obtain the physical parameters for the other two non-pulsating *Kepler* Am stars.

What is certainly clear from Fig. 7 is that there is no relationship between the predicted Am instability strip based on our current understanding of diffusion in these stars, and the actual location of pulsating Am stars. It is true that, as Turcotte et al. (2000) found, the location of the more evolved pulsating δ Del stars are consistent with the predicted instability strip. What we find here is that pulsation in relatively unevolved Am stars appears to be quite common (six of the ten *Kepler* Am stars pulsate) and that this is not currently explained in the context of diffusion.

7 CONCLUSION

We obtained high-resolution spectra of two pulsating Am stars in the *Kepler* field. Such measurements are very important because physical parameters derived from narrow-band photometry may be unreliable. We also find that six of the ten Am stars observed by *Kepler* show δ Sct pulsations (with two showing low-amplitude γ Dor pulsations as well). The other four Am stars do not show any δ Sct pulsations to a level of a few μmag.

We used the spectroscopic estimates of three pulsating *Kepler* Am stars to place these stars in the theoretical HR diagram. The location of most of the other *Kepler* Am stars could be estimated either from the KIC parameters or from $uvby\beta$ photometry and the Balona (1994) calibration. We also investigated all other observations of pulsating Am stars, particularly those with good spectroscopic parameters or with luminosities which could be estimated from the parallax. It is found that the spectral energy distributions constructed using broad-band photometry lead to effective temperatures which are generally in reasonable agreement with the values listed in the *Kepler Input Catalogue* and those from spectroscopy.

The location of these stars in the HR diagram was compared to that of normal δ Sct stars and to the instability strip calculated by Turcotte et al. (2000) from diffusion and pulsation models. We find that there is no obvious difference in the location of the pulsating Am stars and δ Sct stars, though the two constant *Kepler* Am stars that could be placed in the diagram are somewhat hotter than most of the pulsating Am stars. Whereas diffusion models predict that there should be no pulsating Am stars near the ZAMS, we find that many of these stars are, in fact, relatively unevolved. There are also several pulsating Am stars with well-determined parameters that are considerably more luminous and hotter than predicted by pulsating Am-star models. The discrepancy between the observed and calculated instability strips for these stars suggest that our concept of the interaction between pulsation and diffusion in these stars needs to be revised.

ACKNOWLEDGMENTS

The authors wish to thank the *Kepler* team for their generosity in allowing the data to be released to the Kepler Asteroseismic Science Consortium (KASC) ahead of public release and for their outstanding efforts which have made these results possible. Funding for the *Kepler* mission is provided by NASA's Science Mission Directorate.

This work was partially supported by the Italian ESS project, contract ASI/INAF I/015/07/0, WP 03170. We wish to thank the director of Telescopio Nazionale Galileo for the observing time provided us under the Director Discretionary Time program.

LAB wishes to thank the South African Astronomical Observatory for financial support.

REFERENCES

Abt H. A., 1984, ApJ, 285, 247
Allende Prieto C., Barklem P. S., Lambert D. L., Cunha K., 2004, A&A, 420, 183
Allende Prieto C., Lambert D. L., 1999, A&A, 352, 555
Antoci V., Campante T. L., Tygsen A. O., Handler G., Catanzaro, G., Frasca, A., DeCat P., Lüftinger T., Grigahcène A., Bruntt H., 2010, in preparation
Balona L., Cunha M., Kurtz D., Brandao I. M., Gruberbauer M., Saio H., Ostensen R., Elkin V., Borucki W., Christensen-Dalsgaard J., Kjeldsen H., Koch D., 2010, ArXiv e-prints
Balona L. A., 1994, MNRAS, 268, 119
Burkhart C., Coupry M. F., 1989, A&A, 220, 197
Castelli F., Hubrig S., 2004, A&A, 425, 263
Catanzaro G., Ripepi V., Bernabei S., Marconi M., Balona L., Kurtz D. W., Smalley B., Borucki W. J., Bruntt H., Christensen-Dalsgaard J., Grigahcene A., Kjeldsen H., Koch D. G., Monteiro M. J. P. F. G., Suarez J. C., Szabo R., Uytterhoeven K., 2010, ArXiv e-prints
Dupret M., Grigahcène A., Garrido R., Gabriel M., Scuflaire R., 2005, A&A, 435, 927
Erspamer D., North P., 2003, A&A, 398, 1121
Gratton R. G., Bonanno G., Bruno P., Cali A., Claudi R. U., Cosentino R., Desidera S., Diego F., Farisato G., Martorana G.,

Rebeschini M., Scuderi S., 2001, Experimental Astronomy, 12, 107
Grevesse N., Asplund M., Sauval A. J., Scott P., 2010, Ap&SS, 328, 179
Grigahcène A., Antoci V., Balona L., Catanzaro G., Daszyńska-Daszkiewicz J., Guzik J. A., Handler G., Houdek G., Kurtz D. W., Marconi M., Monteiro M. J. P. F. G., Moya A., Ripepi V., Suárez J., Uytterhoeven K., Borucki W. J., Brown T. M., Christensen-Dalsgaard J., Gilliland R. L., Jenkins J. M., Kjeldsen H., Koch D., Bernabei S., Bradley P., Breger M., Di Criscienzo M., Dupret M., García R. A., García Hernández A., Jackiewicz J., Kaiser A., Lehmann H., Martín-Ruiz S., Mathias P., Molenda-Żakowicz J., Nemec J. M., Nuspl J., Paparó M., Roth M., Szabó R., Suran M. D., Ventura R., 2010, ApJ, 713, L192
Henry G. W., Fekel F. C., 2005, AJ, 129, 2026
Hohle M. M., Neuhauser R., Schutz B. F., 2010, VizieR Online Data Catalog, 1133, 10349
Jenkins J. M., Caldwell D. A., Chandrasekaran H., Twicken J. D., Bryson S. T., Quintana E. V., Clarke B. D., Li J., Allen C., Tenenbaum P., Wu H., Klaus T. C., Middour C. K., Cote M. T., McCauliff S., Girouard F. R., Gunter J. P., Wohler B., Sommers J., Hall J. R., Uddin A. K., Wu M. S., Bhavsar P. A., Van Cleve J., Pletcher D. L., Dotson J. A., Haas M. R., Gilliland R. L., Koch D. G., Borucki W. J., 2010, ApJ, 713, L87
Joshi S., Girish V., Sagar R., Kurtz D. W., Martinez P., Kumar B., Seetha S., Ashoka B. N., Zhou A., 2003, MNRAS, 344, 431
Joshi S., Mary D. L., Martinez P., Kurtz D. W., Girish V., Seetha S., Sagar R., Ashoka B. N., 2006, A&A, 455, 303
King H., Matthews J. M., Row J. F., Cameron C., Kuschnig R., Guenther D. B., Moffat A. F. J., Rucinski S. M., Sasselov D., Walker G. A. H., Weiss W. W., 2006, Communications in Asteroseismology, 148, 28
Koch D. G., Borucki W. J., Basri G., Batalha N. M., Brown T. M., Caldwell D., Christensen-Dalsgaard J., Cochran W. D., DeVore E., Dunham E. W., Gautier III T. N., Geary J. C., Gilliland R. L., Gould A., Jenkins J., Kondo Y., Latham D. W., Lissauer J. J., Marcy G., Monet D., Sasselov D., Boss A., Brownlee D., Caldwell J., Dupree A. K., Howell S. B., Kjeldsen H., Meibom S., Morrison D., Owen T., Reitsema H., Tarter J., Bryson S. T., Dotson J. L., Gazis P., Haas M. R., Kolodziejczak J., Rowe J. F., Van Cleve J. E., Allen C., Chandrasekaran H., Clarke B. D., Li J., Quintana E. V., Tenenbaum P., Twicken J. D., Wu H., 2010, ArXiv e-prints
Koen C., Kurtz D. W., Gray R. O., Kilkenny D., Handler G., Van Wyk F., Marang F., Winkler H., 2001, MNRAS, 326, 387
Kurtz D. W., 1978, ApJ, 221, 869
—, 1984, MNRAS, 206, 253
—, 1989, MNRAS, 238, 1077
Kurucz R., Bell B., 1995, Atomic Line Data (R.L. Kurucz and B. Bell) Kurucz CD-ROM No. 23. Cambridge, Mass.: Smithsonian Astrophysical Observatory, 1995., 23
Kurucz R. L., 1993, in Astronomical Society of the Pacific Conference Series, Vol. 44, IAU Colloq. 138: Peculiar versus Normal Phenomena in A-type and Related Stars, M. M. Dworetsky, F. Castelli, & R. Faraggiana, ed., pp. 87–+
Kurucz R. L., Avrett E. H., 1981, SAO Special Report, 391
Martinez P., Kurtz D. W., Ashoka B. N., Chaubey U. S., Girish V., Gupta S. K., Joshi S., Kasturirangan K., Sagar R., Seetha S., 2001, A&A, 371, 1048
Pollacco D. L., Skillen I., Cameron A. C., Christian D. J., Hellier C., Irwin J., Lister T. A., Street R. A., West R. G., Anderson D., Clarkson W. I., Deeg H., Enoch B., Evans A., Fitzsimmons A., Haswell C. A., Hodgkin S., Horne K., Kane S. R., Keenan F. P., Maxted P. F. L., Norton A. J., Osborne J., Parley N. R., Ryans R. S. I., Smalley B., Wheatley P. J., Wilson D. M., 2006, PASP, 118, 1407
Preston G. W., 1974, ARA&A, 12, 257
Robinson S. E., Ammons S. M., Kretke K. A., Strader J., Wertheimer J. G., Fischer D. A., Laughlin G., 2007, ApJS, 169, 430
Smalley B., Dworetsky M. M., 1993, A&A, 271, 515
Smalley B., Kupka F., 1997, A&A, 328, 349
Torres G., Andersen J., Giménez A., 2010, A&A Rev., 18, 67
Turcotte S., Richer J., Michaud G., Christensen-Dalsgaard J., 2000, A&A, 360, 603
van Leeuwen F., 2007, A&A, 474, 653
Zhiping L., 2000, A&A, 360, 185